Dystrophin-compromised sarcoglycan-δ-knockout diaphragm requires full wild-type embryonic stem cell reconstitution for correction

Joseph M. Vitale[1], Joel S. Schneider[1], Amanda J. Beck[1], Qingshi Zhao[1], Corey Chang[1], Richard Gordan[1], Jennifer Michaels[2], Mantu Bhaumik[3] and Diego Fraidenraich[1,*]

[1]Department of Cell Biology and Molecular Medicine, University of Medicine and Dentistry of New Jersey, New Jersey Medical School, 185 S Orange Ave, MSB G667, Newark, NJ, 07107, USA
[2]Department of Neurology and Neurosciences, University of Medicine and Dentistry of New Jersey, New Jersey Medical School, 185 S Orange Ave, MSB H506, Newark, NJ 07107, USA
[3]Department of Pediatrics, University of Medicine and Dentistry of New Jersey, Robert Wood Johnson Medical School, 89 French Street, Room - 4270, New Brunswick, NJ 08901-1935, USA
*Author for correspondence (fraidedi@umdnj.edu)

Accepted 4 December 2011
Journal of Cell Science 125, 1807–1813

doi: 10.1242/jcs.100537

Summary

Limb-girdle muscular dystrophy-2F (LGMD-2F) is an incurable degenerative muscle disorder caused by a mutation in the sarcoglycan-δ (SGδ)-encoding gene (*SGCD* in humans). The lack of SGδ results in the complete disruption of the sarcoglycan complex (SGC) in the skeletal and cardiac muscle within the larger dystrophin–glycoprotein complex (DGC). The long-term consequences of SG ablation on other members of the DGC are currently unknown. We produced mosaic mice through the injection of wild-type (WT) embryonic stem cells (ESCs) into SGδ-knockout (KO) blastocysts. ESC-derived SGδ was supplied to the sarcolemma of 18-month-old chimeric muscle, which resulted in the restoration of the SGC. Despite SGC rescue, and contrary to previous observations obtained with WT/mdx chimeras (a mouse rescue paradigm for Duchenne muscular dystrophy), low levels of ESC incorporation were insufficient to produce histological corrections in SGδ-KO skeletal muscle or heart. The inefficient process of ESC rescue was more evident in the SGδ-KO diaphragm, which had reduced levels of dystrophin and no compensatory utrophin, and needed almost full WT ESC reconstitution for histological improvement. The results suggest that the SGδ-KO mouse model of LGMD is not amenable to ESC treatment.

Key words: Blastocyst, Chimera, Embryonic stem cells, Muscle, Sarcoglycanopathy

Introduction

Some of the most severe forms of muscular dystrophy (MD) result from various deficiencies of key muscle-stabilizing proteins within the dystrophin–glycoprotein complex (DGC). With the 427 kDa dystrophin protein as its backbone, the DGC provides the framework that connects the cytoskeleton with the extracellur matrix. This large complex is also composed of dystroglycans, dystrobrevins, syntrophins, neuronal nitric oxide synthase (nNOS) and the sarcoglycan complex (SGC) (Straub and Campbell, 1997; O'Brien and Kunkel, 2001; Rando, 2001b). In skeletal and cardiac muscle, the SGC tetramer consists of sarcoglycan (SG)-γ, -α, -β and -δ (Nigro et al., 1996a; Nigro et al., 1996b; Duggan et al., 1997; Duclos et al., 1998; Durbeej et al., 2000). Mutations in any of these four glycosylated single-pass transmembrane proteins result in autosomal recessive limb-girdle muscular dystrophy (LGMD-2C-2F). These sarcoglycanopathies commonly cause progressive muscle weakness and pathological changes characterized by cell infiltration, fibrosis and central nucleation (Ozawa et al., 2005). Overall, the LGMDs are a broad and diverse group of both autosomal and recessive disorders affecting 2.27 per 100,000 people (Norwood et al., 2009).

In the absence of SGδ, such as in LGMD-2F, the remaining sarcoglycan members (α, β and γ) cannot assemble and are quickly degraded before transport from the Golgi (Shi et al., 2004; Draviam et al., 2006). The effect of SGδ ablation on other members of the DGC varies. For example, the lack of SGδ, and the resultant SGC, has been reported to leave dystrophin levels unaltered in both skeletal and cardiac tissues (Hack et al., 2000; Li et al., 2009). However, the absence of SGδ has been shown to reduce nNOS levels and increase its displacement from the sarcolemma (Crosbie et al., 2002).

Although studies with pluripotent stem cells (PSCs), embryonic stem cells (ESCs) and induced pluripotent stem cells (iPSCs) in skeletal muscle are emerging (Tian et al., 2008; Quattrocelli et al., 2011), no studies with PSCs in the skeletal muscle of SGδ-knockout (KO) mice have been reported. Previously, utilizing both forms of PSCs (ESCs and iPSCs), we produced mosaic models of mild and severe Duchenne muscular dystrophy (DMD). This was performed by injecting wild-type (WT) PSCs into mdx (a mouse rescue paradigm for Duchenne muscular dystrophy; DMD), and mdx:utrophin KO blastocysts. Both forms of PSCs were incorporated at low percentages into the resultant chimeras and supplied dystrophin to rescue the mdx but not the mdx:utrophin KO muscle tissue, although in both chimeric models there was a recovery of fat mass. This suggests that other tissues also play a role in the development of MD, and

that the PSCs exert corrections globally (Stillwell et al., 2009; Beck et al., 2011). We wanted to study whether the ESC rescue of DMD accomplished in mdx mice with low chimerism also operated in other models of MD, such as LGMD-2F, which is recapitulated in SGδ-KO mice. We injected R26 ESCs into SGδ-KO blastocysts, to generate WT/SGδ chimeras. Our analysis shows that, unlike mdx, the SGδ-KO model is not corrected unless the muscle contained more than half of WT mosaicism. The ESC rescue compromise was more evident in the SGδ-KO diaphragm, which had reduced levels of dystrophin and no compensatory utrophin, and needed almost full WT ESC reconstitution for histological improvement.

Results

To generate WT/SGδ chimeric mice, we injected WT *lacZ*-marked R26 ESCs into SGδ-KO blastocysts. At 3 weeks of age, the degree of ESC incorporation, or chimerism, was estimated by performing X-gal staining of sections of tail biopsies and semi-quantitative (semi-Q) genomic PCR for both the WT and mutant SGδ genes, as described previously (Stillwell et al., 2009; Beck et al., 2011). We analyzed four mice with <5% ESC incorporation, one mouse with 10% incorporation, two with 40–60% incorporation and two with 60–80% incorporation. In 18-month-old mice, the degree of chimerism was reconfirmed by X-gal staining of the older tail biopsies, by semi-Q genomic PCR (supplementary material Fig. S1), and by immunofluorescence analysis of the heart for the SGC (supplementary material Fig. S2Q–T) (Stillwell et al., 2009; Beck et al., 2011).

WT/SGδ muscle does not show histological corrections with <60% ESC incorporation

We evaluated the histopathological consequences of the ESC treatment in the muscle of 18-month-old chimeras. In chimeras with <60% ESC reconstitution, the skeletal muscle (diaphragm, quadriceps and pectoralis) exhibited a dystrophic phenotype. Along with disorganized fiber architecture, these tissues had more fibrosis (Fig. 1G,H,K,L,O,P), central nucleation (Table 1; Fig. 2G,H,K,L,O,P) and mononuclear invasion (Fig. 2G,H,K,L) relative to WT. With >60% ESC incorporation, the quadriceps and pectoralis both took on a WT-like phenotype, with little or no fibrosis (Fig. 1J,N), uniform fiber sizes (Fig. 2J,N) and little or no central nucleation (Table 1; Fig. 2J,N). However, the diaphragm was not rescued with >60% ESC incorporation as it still showed fibrosis (Fig. 1F) and more central nucleation (Table 1; Fig. 2F) relative to WT, but less mononuclear invasion than <60% chimeric diaphragm (compare Fig. 2F with 2G).

Unlike the skeletal muscle, the heart does not syncytialize. However, similar to the pectoralis and quadriceps, the heart was also rescued with >60% ESC mosaicism (Fig. 1B for interstitial fibrosis; Fig. 2B for mononuclear invasion), although fibrosis at the periphery of the blood vessels still remained (compare Fig. 1B with 1A). This cardiac improvement was supported by functional echocardiogram data [the ejection fraction (EF) of 40–60%, 10–20% and <5% WT/SGδ hearts was 58.2±3.97 (n=6) compared with the EF of 60–80% WT/SGδ and WT hearts, which was 68.3±6.45 (n=4; values are means±s.e.m.; P<0.05)].

The skeletal muscle but not the heart of 60–80% WT/SGδ chimeras has uniform SGC distribution

We ascertained whether ESCs restore the SGC in skeletal muscle and heart. SGδ-KO mice have been shown to have complete ablation of the SGC with no residual sarcoglycan expression (Hack et al., 2000; Draviam et al., 2006). Similar to SGδ-KO, immunofluorescence analysis showed a lack of expression of SGβ and SGα in the <5% chimeras (supplementary material Fig. S2D,H,L,P,T). In 40–60% WT/SGδ chimeras, clusters of SGα− and SGβ-positive cardiomyocytes and skeletal muscle fibers appeared, indicating the reinstatement of the SGC, albeit in patches throughout the tissue (supplementary material Fig. S2C,G,K,O,S). When the ESC incorporation was increased in the 60–80% WT/SGδ chimeras, the SGC was uniformly restored nearly to, or at, WT levels in the skeletal muscle (supplementary material Fig. S2B,F,J,N). However, the heart (non-syncytium) of 60–80% WT/SGδ chimeras had few patches of muscle unstained (supplementary material Fig. S2R). In spite of the abundance

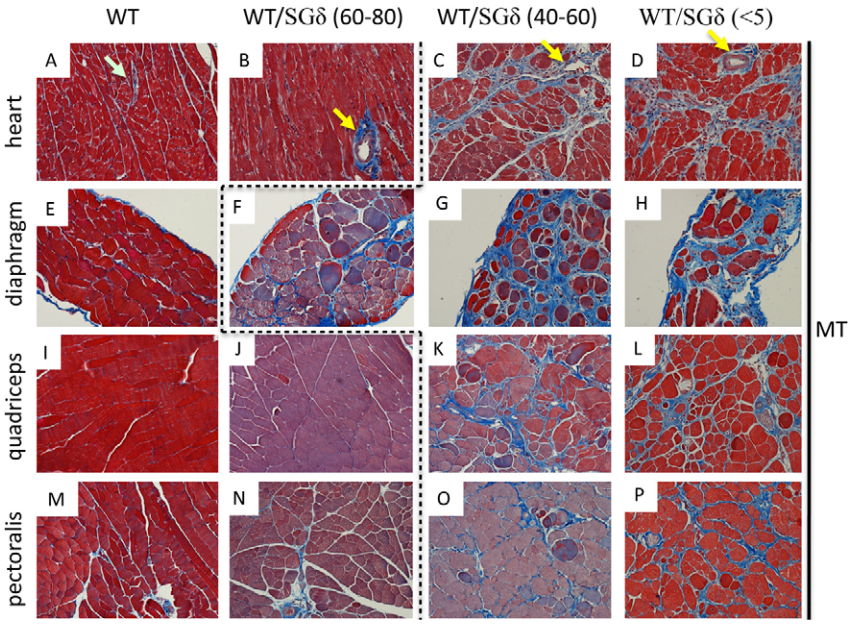

Fig. 1. WT ESC incorporation does not prevent fibrosis in WT/SGδ chimeras with less than 60% mosaicism. Heart (**A–D**), diaphragm (**E–H**), quadriceps (**I–L**) and pectoralis (**M–P**) muscles were paraffin sectioned and Masson trichrome (MT) stained. WT (A,E,I,M), 60–80% WT/SGδ (B,F,J,N), 40–60% WT/SGδ (C,G,K,O) and <5% WT/SGδ (D,H,L,P) chimeras were analyzed. Yellow arrows (B–D) denote vascular-associated fibrosis. Light blue arrow (A) denotes no vascular–associated fibrosis. The dashed line separates non–phenotypic (left of line) from phenotypic (right of line) tissues. Original magnification 200× (A–D); 100× (E–P).

Table 1. Central nucleation values for chimeric skeletal muscles

		WT/SGδ chimeras (*n*)		
Muscle	WT (*n*)	60–80%	40–60%	<5%
Diaphragm	7±3 (3)	15±3* (5)	15±4* (5)	14±3* (5)
Quadriceps	1±1 (3)	8±8‡ (4)	51±7* (4)	51±7* (4)
Pectoralis	5±3 (3)	4±3‡ (3)	88±1* (4)	82±3* (5)

Values are means ± s.e.m.; *n*, number of sections.
*$P<0.05$ relative to WT; ‡$P>0.05$ relative to WT.

of SGC-stained areas in 60–80% diaphragm (supplementary material Fig. S2J,N), this muscle had dystrophic features (Fig. 1F; Fig. 2F).

We determined that SGδ protein levels in the chimeric muscle also correlated with the observed SGC restoration. There was a recovery of SGδ in the 60–80% chimeras and to a lesser extent in the <60% chimeras, although there was a noticeable protein band just below the normal SGδ band (Fig. 3A–D). This lower molecular mass band is more prominent in 60–80% chimeras than in WT.

The WT/SGδ chimera diaphragm shows lower dystrophin levels but no utrophin upregulation

Dystrophin has previously been found to be unaffected by the loss of the SGC (Hack et al., 2000; Li et al., 2009). In our previous models with mdx mice, there was a noticeable lack of uniformity of dystrophin-positive fibers within the rescued muscle (Stillwell et al., 2009; Beck et al., 2011). However, in WT/SGδ chimeras, dystrophin was detected in all fibers, but its overall staining intensity appeared to vary (Fig. 4). In the pectoralis, there appeared to be minimal differences in dystrophin staining intensity in WT, KO and chimeras, irrespective of the degree of mosaicism (Fig. 4A–D). By contrast, the staining intensity of dystrophin in the diaphragm varied with the percentage chimerism, although there was some residual dystrophin staining in every fiber (Fig. 4E–H). Western blot analysis also showed this observed dystrophin reduction in the diaphragms of the chimeras (Fig. 3C). Dystrophin levels in the diaphragm of <5% chimeras were 12.5-times reduced compared with WT (supplementary material Fig.S3). Despite the fact that dystrophin levels were severely reduced (but not absent) in the diaphragm of SGδ-KO or <5% WT/SGδ chimeras (compare Fig. 4H with 4D; and Fig. 3C with 3A), we found no upregulation of the dystrophin homologue utrophin (Fig. 5), ultimately putting the dystrophic tissue at an even greater risk for injury.

Deficiencies in SGδ decrease nNOS levels in the skeletal muscle but not in the heart of WT/SGδ mice

We determined whether the loss of SGδ and the SGC affects nNOS expression in the WT/SGδ chimeras. We observed overall lower levels of nNOS in skeletal muscle (pectoralis, quadriceps and diaphragm) that correlated with the level of chimerism (Fig. 6A–C). At the sarcolemma, nNOS associates with the DGC through dystrophin and syntrophin (Miyagoe-Suzuki and Takeda, 2001; Lai et al., 2009). Although the pectoralis and quadriceps did not show any noticeable decrease in dystrophin or in syntrophin (Fig. 3A–B; Fig. 6A–B), the diaphragm had lower levels of dystrophin, but not syntrophin (Fig. 3C; Fig. 6C). Thus, nNOS levels were compromised in the SGδ-KO and SGδ non-rescued chimeras irrespective of the lack of changes observed in dystrophin or syntrophin levels.

Although in the hearts of chimeras the levels of SGδ were lower than in WT (Fig. 3D), this was not so for dystrophin, syntrophin or nNOS (Fig. 3D; Fig. 6D). The lack of reduction observed in nNOS levels could probably be attributed to the lack of any major disruption of the DGC, or to the presence of nNOS isoforms not directly associated with the DGC in cardiac tissue (Li et al., 2010; Percival et al., 2010), in contrast to the main sarcolemmal nNOS found in skeletal muscle (Mungrue and Bredt, 2004).

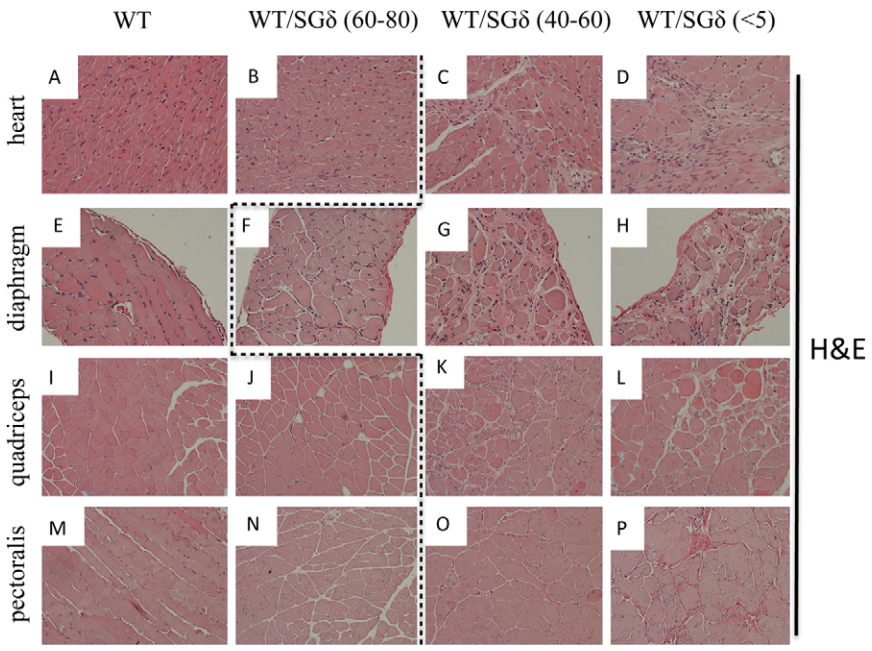

Fig. 2. WT ESC incorporation does not prevent mononuclear invasion and central nucleation in WT/SGδ chimeras with less than 60% mosaicism. Heart (**A–D**), diaphragm (**E–H**), quadriceps (**I–L**) and pectoralis (**M–P**) were paraffin sectioned and Hematoxylin and Eosin stained. WT (A,E,I,M), 60–80% WT/SGδ (B,F,J,N), 40–60% WT/SGδ (C,G,K,O) and <5% WT/SGδ (D,H,L,P) were analyzed. The dashed line separates non–phenotypic (left of line) from phenotypic (right of line) tissues. Original magnification 200× (A–D); 100× (E–P).

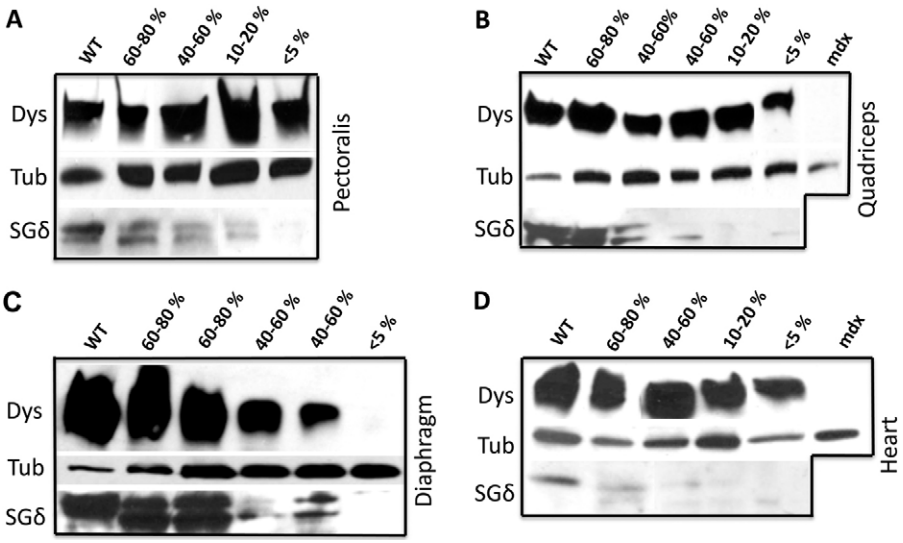

Fig. 3. Dystrophin levels are compromised in the diaphragm of WT/SGδ chimeras. Protein extracts from pectoralis (**A**), quadriceps (**B**), diaphragm (**C**) and heart (**D**) of 18-month-old WT, 60–80% WT/SGδ, 40–60% WT/SGδ, 10–20% WT/SGδ, <5% WT/SGδ and mdx mice were subjected to western blot for dystrophin (Dys), SGδ and tubulin (Tub).

Discussion

We have shown that it takes over 60% WT ESC chimerism for the rescue of all but the diaphragm of LGMD-2F mice. However, in previous reports, we showed that it takes approximately10–30% ESC (or iPSC) incorporation to rescue mdx mice, which are predisposed to DMD (Stillwell et al., 2009; Beck et al., 2011). This disparity could be because of several factors linked to differences between the mdx and SGδ-KO MD mouse models and/or with their respective interactions with the ESCs. The ESCs might over-produce dystrophin (Stillwell et al., 2009) but not SGδ in the rescue of their respective MD mouse models. Likewise, the ESCs might overproduce dystrophin in mdx (Stillwell et al., 2009) but not in SGδ-KO mice. The mdx mouse shows histological lesions typical of MD, but muscular wastage proceeds in a much milder fashion compared with human DMD (Willmann et al., 2009). These differences between humans and mice have been attributed in part to an increased regenerative capacity of muscle in mice (Pastoret and Sebille, 1995; Sacco et al., 2010). In mdx mice and DMD, dystrophin-deficient tissues are partially compensated for through the upregulation of the dystrophin homologue utrophin, however inefficiently (Deconinck et al., 1997), and mouse muscle without dystrophin and utrophin cannot be rescued with low WT pluripotent stem cell chimerism (Beck et al., 2011). Utrophin is overexpressed in the sarcolemma of mdx mice, but not in SGδ-KO mice (Li et al., 2009) or WT/SGδ chimeras (Fig. 5). Consequently, when dytrophin levels decrease in the diaphragm of the WT/SGδ chimeras, there is no utrophin to help compensate. Unlike mdx tissue, there is residual dystrophin in the fibers of our WT/SGδ chimeras. This threshold of residual sarcolemmal dystrophin is probably sufficient to negatively inhibit utrophin upregulation, because sarcolemmal dystrophin inhibits sarcolemmal utrophin (Beck et al., 2011). Lack of SGδ, combined with dystrophin reduction and absence of sarcolemmal utrophin would cause the tissue to be highly susceptible to stress-induced damage, mononuclear invasion and fibrosis.

In all the four chimeric tissues we examined, we observed in western blots that there were double bands, of approximately 35 kDa, for SGδ. This is consistent with the fact that there are several SGδ isoforms in skeletal muscle and fat (Estrada et al., 2006; Groh et al., 2009). However, this finding contrasts with previous published data (Li et al., 2009) showing one major band for SGδ although the previous studies were performed with muscle from non-aging mice. We believe that the use of a gradient polyacrylamide gel also contributes to the resolution of SGδ isoforms in the range of 30–40 kDa. Although the higher molecular mass band roughly paralleled the degree of mosaicism, the lower molecular mass band was more prominent in the chimeric than in the WT tissue. We showed that a number of dystrobrevin products were prevalent in a non-dystrophic state, and a number of dystrobrevin products were prevalent in a dystrophic state (Stillwell et al., 2009). An association of SGδ

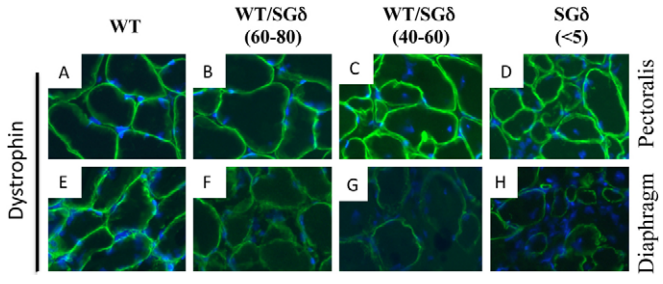

Fig. 4. Sarcolemmal dystrophin is compromised in the diaphragm of WT/SGδ chimeras. Immunofluorescence analysis for dystrophin (green) in the pectoralis (**A**–**D**) and diaphragm (**E**–**H**) of 18-month-old WT (A,E), 60–80% WT/SGδ (B,F), 40–60% WT/SGδ (C,G) and <5% WT/SGδ (D,H) chimeras. Blue staining: DAPI. Original magnification: 400×.

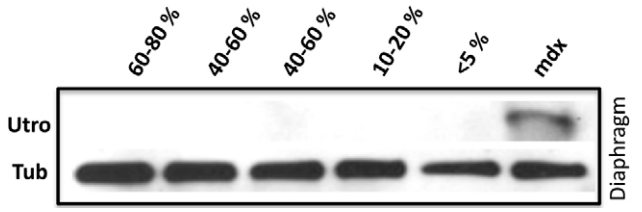

Fig. 5. The WT/SGδ diaphragm does not show upregulation of utrophin. Protein extracts from diaphragms of 18-month-old WT, 60–80% WT/SGδ, 40–60% WT/SGδ, 10–20% WT/SGδ, <5% WT/SGδ and mdx mice were subjected to western blot for utrophin (Utro) and tubulin (Tub).

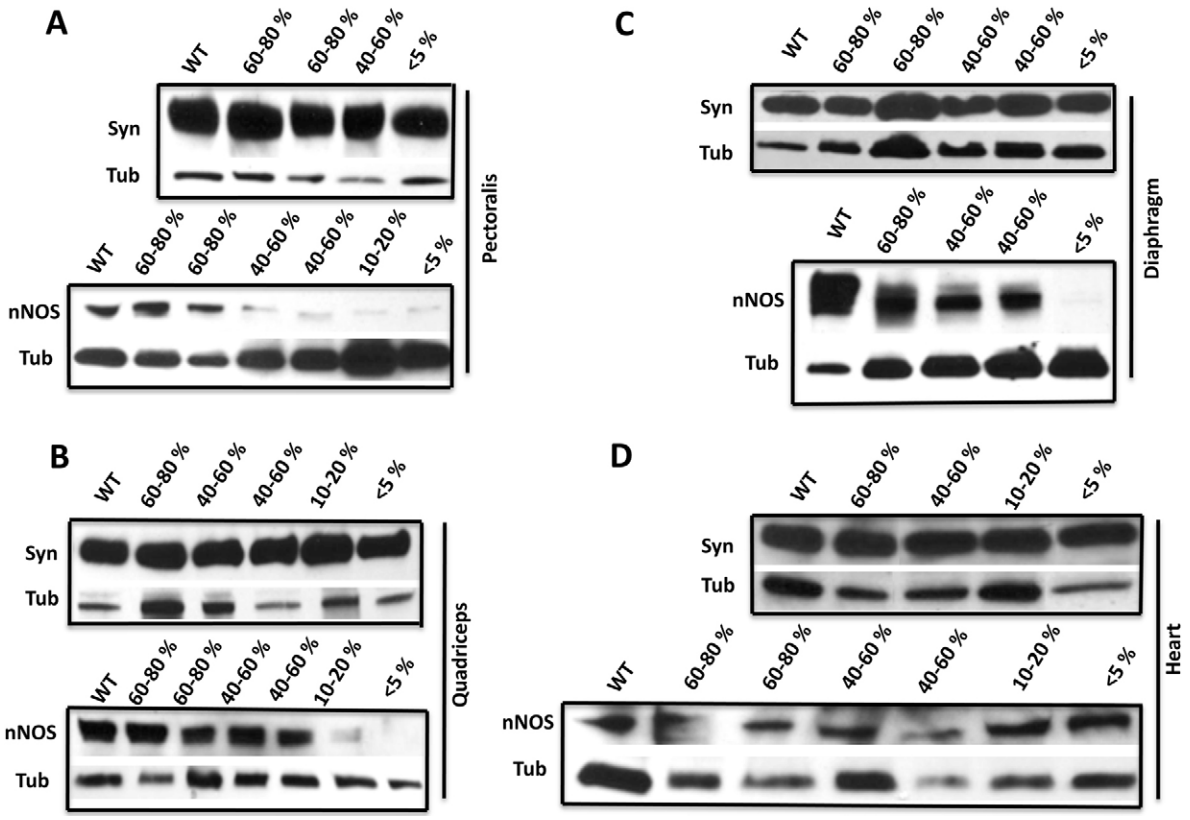

Fig. 6. nNOS levels are compromised in WT/SGδ chimeras. Protein extracts from pectoralis (**A**), quadriceps (**B**), diaphragm (**C**) and heart (**D**) of 18-month-old WT, 60–80% WT/SGδ, 40–60% WT/SGδ, 10–20% WT/SGδ and <5% WT/SGδ mice were subjected to western blot for syntrophin (Syn), nNOS and tubulin (Tub).

products with a chimeric and dystrophic state has not been reported before. The prevalence of a lower (potentially inactive or partially active) molecular mass SGδ product in chimeras could also help explain why more ESC chimerism is needed for correction in SGδ-KO than in mdx mice. We have previously reported the induction of neomorphic effects in chimeras as a result of interactions between WT and mutant environment (Fraidenraich et al., 2004; Zhao et al., 2010). This switch in the pattern of high versus low SGδ molecular mass bands might represent another example of a neomorphic process. Whether this banding pattern corresponds to previously identified functional SGδ isoforms (Estrada et al., 2006), or whether it corresponds to previously unknown products, it remains to be elucidated.

In skeletal muscle, nNOS, which produces nitric oxide, is involved in many downstream effects, including vasodilation, muscle contractility, Ca^{2+} release and glucose uptake (Stamler and Meissner, 2001; Percival et al., 2010; Li et al., 2011). Several mechanisms have been postulated for the association of nNOS with the DGC. One is the PDZ domain observed in both nNOS and α1-syntrophin (Adams et al., 2001). Another is the spectrin-like repeats 16 and 17 in the rod domain of dystrophin (Lai et al., 2009). In the absence of these domains, nNOS fails to be recruited to the sarcolemma, and could be mislocalized and degraded. In a dystrophic environment, high calcium might supra-activate the enzyme (Zhou and Zhu, 2009) present in the non-rescued chimera, which in turn might produce undesirable reactive nitrogen species (RNS), to ultimately alter important downstream processes (Rando, 2001a; Li et al., 2011). This detrimental process could continuously lead to a more pronounced dystrophic environment. It is important to point out that syntrophin levels were not compromised in any muscle analyzed. Although dystrophin reduction can explain nNOS reduction in the diaphragm, the disruption or improper localization of other members (i.e. sarcoglycan and/or dystroglycan loss or syntrophin mislocalization) might have to account for the reduction of nNOS in quadriceps or pectoralis.

It has been previously reported that there are no decreases in dystrophin levels in SGδ or other sarcoglycan-KO mouse models (Hack et al., 2000; Li et al., 2009). However, we report that the lack of the SGC (directly or indirectly) triggers decreases in dystrophin levels in specific muscles. This occurs primarily in the diaphragm, which has unique tissue architecture and a mixed composition of both slow- and fast-twitch fiber types (Kobzik et al., 1994). Moreover, the age of the WT/SGδ chimeras (18-months) could have exacerbated the dependence of dystrophin on the SGC [the age of the examined muscles is relevant to LGMD-2F, as patients do not die in their teens as is the case of DMD (Durbeej and Campbell, 2002; Laval and Bushby, 2004)]. With a severe compromise in dystrophin and no compensatory utrophin, the pathology of the diaphragm in LGMD-2F would become more severe. This severe phenotype, in turn, might detrimentally impinge on the presence of dystrophin (i.e. decreased production or increased destruction), to further intensify the muscle damage. Thus, the presence of the dystrophic fibers, because of an SGC-deficient environment, could produce an amplified destructive process through dystrophin reduction. This cascading scenario

could ultimately lead to increased resistance to ESC treatment. However, we cannot formally rule out the opposite scenario, in which the severe phenotype acts as the primary trigger for the observed decreases in dystrophin. Nevertheless, the study shows a tight correlation between dystrophy and dystrophin reduction in specific muscles of SGδ-KO mice.

In conclusion, we describe here that, unlike mdx, the SGδ-KO model is not amenable to ESC-treatment, particularly the diaphragm. Our results argue against the concept that every MD paradigm could be easily treatable with ESCs. Furthermore, the syncytial nature of the skeletal muscle has to be regarded as a facilitator for DGC reconstitution in ESC therapy, but this prevailing concept might have to be revisited, because the SGδ-KO heart, which does not syncytialize, requires a similar (high) threshold for ESC correction to that of the SGδ-KO pectoralis/quadriceps.

Materials and Methods

Embryonic stem cells

WT *lacZ*-marked Rosa 26 (R26) mouse ESCs were provided by Phillipe Soriano (Mount Sinai School of Medicine, New York, NY). R26 ESCs grow in KO-DMEM, 15% ESC-grade FBS, 1% glutamine, 1% penicillin and streptomycin, 1% non-essential amino acids, 1% nucleosides, β-mercaptoethanol and leukemia inhibitory factor (LIF). ESCs were cultured on top of murine embryonic fibroblasts in a gelatin-coated plate.

Generation of chimeric mice

SGδ-KO females (3 weeks old) were superovulated by intraperitoneal injection with chorionic gonadotrophin and gonadotrophin (Calbiochem, Darmstadt, Germany), 3 days and 1 day, respectively, before mating with SGδ-KO stud males. After 3.5 days, the females were killed and the uteri were flushed in order to collect blastocysts. Each blastocyst was then microinjected with 12–15 WT R26 ESCs. Then the chimeric blastocysts were implanted into the uteri of pseudopregnant surrogate females and the pregnancy was allowed to develop to term. All mice were killed at 18 months of age. All animal experiments were conducted in accordance and with the approval by the Institutional Animal Care and Use Committee (IACUC) of the University of Medicine and Dentistry of New Jersey.

Western blotting

Tissue was homogenized in lysis buffer and protein concentrations were determined using the BCA™ Protein Assay Kit (Thermo Scientific, Rockford, IL). For gel electrophoresis, a 4–20% gradient acrylamide (Ready Gels, Bio-Rad, Hercules, CA) was used and 40 µg of protein were loaded per well. PVDF membranes were blotted with antibodies specific for dystrophin (dys1, 1:250; Novocastra, Leica Microsystems, Buffalo Grove, IL), syntrophin (1:100; Thermo Scientific), nNOS (1:2500; Thermo Scientific), sarcoglycan-δ (1:200; Santa Cruz Biotechnology, Santa Cruz, CA), Utrophin (1:200; MANCHO3, clone 8a4s, Developmental Studies Hybridoma Bank, University of Iowa, IA) and α-tubulin (1:10,000; Abcam, Cambridge, MA). High molecular mass protein standards (PageRuler, Fermentas, Burlington, ON, Canada) were used. The intensities of the western blot exposures were quantified using Quantity One software on a GS800-Densitometer (Bio-Rad). The relative expression levels for the dystrophin bands were normalized using tubulin bands within the same linear range of detection using Quantity One® 1-D analysis software. Four scans ($n=4$) per tissue were used to calculate the mean relative expression level for dystrophin and these values were adjusted to scale. Values obtained from WT samples were arbitrarily assigned values of 1.

Immunofluorescence and X-gal histochemistry

Mice were killed at 18 months of age and tissues were harvested. Samples were embedded in OCT and then cryosectioned (10 µm). For immunofluorescence, the cryosections were stained with antibodies specific for dystrophin (1:20, dys2; Novocastra), sarcoglycan-α (1:200; Novocastra) and sarcoglycan-β (1:200; Novocastra). Cryosections were also used for X-gal histochemistry. The X-gal staining solution consisted of 1 mg/ml of X-gal in PBS buffer containing 5 mM potassium ferricyanide, 5 mM potassium ferrocyanide and 2 mM $MgCl_2$. Slides were incubated overnight at 37℃ and then counterstained with Eosin the next day.

Histology

Chimeric and control mice were killed at 18 months of age and tissues were harvested. Samples were fixed in 4% paraformaldehyde and embedded before undergoing Hematoxylin and Eosin (H and E), and Masson trichrome (MT) staining. Digital images of skeletal and cardiac muscle sections were obtained using a Cool SNAP ES2 camera attached to a Nikon Eclipse 80i upright microscope. Central nucleation values were obtained by counting fibers that were centrally nucleated on Hematoxylin and Eosin-stained sections of pectoralis, quadriceps and diaphragm. Sections from similar regions of the tissues were chosen for a more accurate assessment.

Semi-quantitative genomic PCR

Genomic DNA from all chimeras, WT and SGδ controls was isolated from tail snips by overnight digestion in SDS and proteinase K buffer followed by phenol–chloroform extraction. For PCR, 50 ng of genomic DNA was used with primers for genotyping the WT allele of SGδ (primers: forward 5′-gcaaacttggagagtgaagaggc-3′ and reverse 5′-gaggcatataaagtttgcacgac-3′) and the mutant allele of SGδ (primers: forward 5′-gcaaacttggagagtgaagaggc-3′ and reverse 5′-tctatagatctatagatctctcgtgg-3′). 2 ng of the same DNA was used in PCR with Id1 (Fraidenraich et al., 2004) and GAPDH control primers (Clontech) were used as the internal control. PCR was performed with puReTaq Ready-To-Go PCR beads (GE Healthcare, Chalfont St Giles, UK) in the log phase (using 30–35 cycles). Scans were performed on a Typhoon 8600 Variable Mode Imager (Molecular Dynamics, Sunnyvale, CA), and quantified using ImageQuant.

Echocardiography

Echocardiographs were performed on 18-month-old chimeras and WT controls to determine the left ventricular (LV) systolic fraction. Mice were anesthetized by intraperitoneal injection of 2.5% Avertin (290 mg/kg). Transthoracic echocardiography (Sequoia C256; Acuson, Mountain View, CA) was performed using a 13 MHz linear ultrasound transducer. The chest was shaved and the mouse was placed on a warm saline bag in a shallow left lateral position, and warm coupling gel applied to the chest. Small-needle electrocardiographic leads were attached to each limb. Two-dimensional images and LV M-mode tracing (sweep speed of 100–200 mm/second) were recorded from the parasternal short-axis view at the mid papillary muscle level. M-mode measurements of LV internal diameter (LVID) and wall thicknesses were made of three consecutive beats, and averaged using the leading edge-to-leading edge convention adopted by the American Society of Echocardiography. End-diastolic measurements were taken at the peak of the R wave of the electrocardiogram. End-systolic measurements were made at the time of the most anterior systolic excursion of the posterior wall. The LV ejection fraction (EF) was calculated by the cubed methods as follows: $\text{LVEF}\ (\%)=100[(\text{LVID}_d)3-(\text{LVID}_s)3]/(\text{LVID}_d)3$, where d indicates diastolic and s indicates systolic.

Statistical analysis

Data are presented as a means ± standard error of mean (s.e.m.). Statistical analysis was performed with the SPSS software (SPSS, Chicago, IL). For single group comparisons, statistical analysis was determined by unpaired *t*-tests. For multiple group comparisons, statistical analysis was determined by one-way ANOVAs followed by Bonferroni post-hoc analyses. The probability value of <0.05 was considered to be statistically significant.

Acknowledgements

We thank Kevin Campbell for providing the SGδ-KO mouse line, J. and P. Jetko (Cell Biology Histology Core at the University of Medicine and Dentistry of New Jersey) for sectioning and S. Gao for echocardiography. Chimeric mice were generated at the Transgenic and Knockout Mouse Shared Resource of University of Medicine and Dentistry of New Jersey, Robert Wood Johnson Medical School, Cancer Institute of New Jersey.

Funding

This work was supported by the Muscular Dystrophy Association [grant number 200037 to D.F.]; the National Institutes of Health [grant numbers R21-HL094905 to D.F. and T31-HL069752 to students J.M.V. and J.S.S.]; and by the Department of Cell Biology and Molecular Medicine, University of Medicine and Dentistry of New Jersey - New Jersey Medical School start-up funds to D.F. Deposited in PMC for release after 12 months.

Supplementary material available online at
http://jcs.biologists.org/lookup/suppl/doi:10.1242/jcs.100537/-/DC1

References

Adams, M. E., Mueller, H. A. and Froehner, S. C. (2001). In vivo requirement of the alpha-syntrophin PDZ domain for the sarcolemmal localization of nNOS and aquaporin-4. *J. Cell Biol.* **155**, 113-122.

Beck, A. J., Vitale, J. M., Zhao, Q., Schneider, J. S., Chang, C., Altaf, A., Michaels, J., Bhaumik, M., Grange, R. and Fraidenraich, D. (2011). Differential requirement for utrophin in the induced pluripotent stem cell correction of muscle versus fat in muscular dystrophy mice. *PLoS One* **6**, e20065.

Crosbie, R. H., Barresi, R. and Campbell, K. P. (2002). Loss of sarcolemma nNOS in sarcoglycan-deficient muscle. *FASEB J.* **16**, 1786-1791.

Deconinck, A. E., Rafael, J. A., Skinner, J. A., Brown, S. C., Potter, A. C., Metzinger, L., Watt, D. J., Dickson, J. G., Tinsley, J. M. and Davies, K. E. (1997). Utrophin-dystrophin-deficient mice as a model for Duchenne muscular dystrophy. *Cell* **90**, 717-727.

Draviam, R. A., Shand, S. H. and Watkins, S. C. (2006). The beta-delta-core of sarcoglycan is essential for deposition at the plasma membrane. *Muscle Nerve* **34**, 691-701.

Duclos, F., Straub, V., Moore, S. A., Venzke, D. P., Hrstka, R. F., Crosbie, R. H., Durbeej, M., Lebakken, C. S., Ettinger, A. J., van der Meulen, J. et al. (1998). Progressive muscular dystrophy in alpha-sarcoglycan-deficient mice. *J. Cell Biol.* **142**, 1461-1471.

Duggan, D. J., Manchester, D., Stears, K. P., Mathews, D. J., Hart, C. and Hoffman, E. P. (1997). Mutations in the delta-sarcoglycan gene are a rare cause of autosomal recessive limb-girdle muscular dystrophy (LGMD2). *Neurogenetics* **1**, 49-58.

Durbeej, M. and Campbell, K. P. (2002). Muscular dystrophies involving the dystrophin-glycoprotein complex: an overview of current mouse models. *Curr. Opin. Genet. Dev.* **12**, 349-361.

Durbeej, M., Cohn, R. D., Hrstka, R. F., Moore, S. A., Allamand, V., Davidson, B. L., Williamson, R. A. and Campbell, K. P. (2000). Disruption of the beta-sarcoglycan gene reveals pathogenetic complexity of limb-girdle muscular dystrophy type 2E. *Mol. Cell* **5**, 141-151.

Estrada, F. J., Mornet, D., Rosas-Vargas, H., Angulo, A., Hernandez, M., Becker, V., Rendon, A., Ramos-Kuri, M. and Coral-Vazquez, R. M. (2006). A novel isoform of delta-sarcoglycan is localized at the sarcoplasmic reticulum of mouse skeletal muscle. *Biochem. Biophys. Res. Commun.* **340**, 865-871.

Fraidenraich, D., Stillwell, E., Romero, E., Wilkes, D., Manova, K., Basson, C. T. and Benezra, R. (2004). Rescue of cardiac defects in id knockout embryos by injection of embryonic stem cells. *Science* **306**, 247-252.

Groh, S., Zong, H., Goddeeris, M. M., Lebakken, C. S., Venzke, D., Pessin, J. E. and Campbell, K. P. (2009). Sarcoglycan complex: implications for metabolic defects in muscular dystrophies. *J. Biol. Chem.* **284**, 19178-19182.

Hack, A. A., Lam, M. Y., Cordier, L., Shoturma, D. I., Ly, C. T., Hadhazy, M. A., Hadhazy, M. R., Sweeney, H. L. and McNally, E. M. (2000). Differential requirement for individual sarcoglycans and dystrophin in the assembly and function of the dystrophin-glycoprotein complex. *J. Cell Sci.* **113**, 2535-2544.

Kobzik, L., Reid, M. B., Bredt, D. S. and Stamler, J. S. (1994). Nitric oxide in skeletal muscle. *Nature* **372**, 546-548.

Lai, Y., Thomas, G. D., Yue, Y., Yang, H. T., Li, D., Long, C., Judge, L., Bostick, B., Chamberlain, J. S., Terjung, R. L. et al. (2009). Dystrophins carrying spectrin-like repeats 16 and 17 anchor nNOS to the sarcolemma and enhance exercise performance in a mouse model of muscular dystrophy. *J. Clin. Invest.* **119**, 624-635.

Laval, S. H. and Bushby, K. M. (2004). Limb-girdle muscular dystrophies – from genetics to molecular pathology. *Neuropathol. Appl. Neurobiol.* **30**, 91-105.

Li, D., Long, C., Yue, Y. and Duan, D. (2009). Sub-physiological sarcoglycan expression contributes to compensatory muscle protection in mdx mice. *Hum. Mol. Genet.* **18**, 1209-1220.

Li, D., Bareja, A., Judge, L., Yue, Y., Lai, Y., Fairclough, R., Davies, K. E., Chamberlain, J. S. and Duan, D. (2010). Sarcolemmal nNOS anchoring reveals a qualitative difference between dystrophin and utrophin. *J. Cell Sci.* **123**, 2008-2013.

Li, D., Yue, Y., Lai, Y., Hakim, C. H. and Duan, D. (2011). Nitrosative stress elicited by nNOSmicro delocalization inhibits muscle force in dystrophin-null mice. *J. Pathol.* **223**, 88-98.

Miyagoe-Suzuki, Y. and Takeda, S. I. (2001). Association of neuronal nitric oxide synthase (nNOS) with alpha1-syntrophin at the sarcolemma. *Microsc. Res. Tech.* **55**, 164-170.

Mungrue, I. N. and Bredt, D. S. (2004). nNOS at a glance: implications for brain and brawn. *J. Cell Sci.* **117**, 2627-2629.

Nigro, V., de Sa Moreira, E., Piluso, G., Vainzof, M., Belsito, A., Politano, L., Puca, A. A., Passos-Bueno, M. R. and Zatz, M. (1996a). Autosomal recessive limb-girdle muscular dystrophy, LGMD2F, is caused by a mutation in the delta-sarcoglycan gene. *Nat. Genet.* **14**, 195-198.

Nigro, V., Piluso, G., Belsito, A., Politano, L., Puca, A. A., Papparella, S., Rossi, E., Viglietto, G., Esposito, M. G., Abbondanza, C. et al. (1996b). Identification of a novel sarcoglycan gene at 5q33 encoding a sarcolemmal 35 kDa glycoprotein. *Hum. Mol. Genet.* **5**, 1179-1186.

Norwood, F. L., Harling, C., Chinnery, P. F., Eagle, M., Bushby, K. and Straub, V. (2009). Prevalence of genetic muscle disease in Northern England: in-depth analysis of a muscle clinic population. *Brain* **132**, 3175-3186.

O'Brien, K. F. and Kunkel, L. M. (2001). Dystrophin and muscular dystrophy: past, present, and future. *Mol. Genet. Metab.* **74**, 75-88.

Ozawa, E., Mizuno, Y., Hagiwara, Y., Sasaoka, T. and Yoshida, M. (2005). Molecular and cell biology of the sarcoglycan complex. *Muscle Nerve* **32**, 563-576.

Pastoret, C. and Sebille, A. (1995). mdx mice show progressive weakness and muscle deterioration with age. *J. Neurol. Sci.* **129**, 97-105.

Percival, J. M., Anderson, K. N., Huang, P., Adams, M. E. and Froehner, S. C. (2010). Golgi and sarcolemmal neuronal NOS differentially regulate contraction-induced fatigue and vasoconstriction in exercising mouse skeletal muscle. *J. Clin. Invest.* **120**, 816-826.

Quattrocelli, M., Palazzolo, G., Floris, G., Schoffski, P., Anastasia, L., Orlacchio, A., Vandendriessche, T., Chuah, M. K., Cossu, G., Verfaillie, C. et al. (2011). Intrinsic cell memory reinforces myogenic commitment of pericyte-derived iPSCs. *J. Pathol.* **223**, 593-603.

Rando, T. A. (2001a). Role of nitric oxide in the pathogenesis of muscular dystrophies: a "two hit" hypothesis of the cause of muscle necrosis. *Microsc. Res. Tech.* **55**, 223-235.

Rando, T. A. (2001b). The dystrophin-glycoprotein complex, cellular signaling, and the regulation of cell survival in the muscular dystrophies. *Muscle Nerve* **24**, 1575-1594.

Sacco, A., Mourkioti, F., Tran, R., Choi, J., Llewellyn, M., Kraft, P., Shkreli, M., Delp, S., Pomerantz, J. H., Artandi, S. E. et al. (2010). Short telomeres and stem cell exhaustion model Duchenne muscular dystrophy in mdx/mTR mice. *Cell* **143**, 1059-1071.

Shi, W., Chen, Z., Schottenfeld, J., Stahl, R. C., Kunkel, L. M. and Chan, Y. M. (2004). Specific assembly pathway of sarcoglycans is dependent on beta- and delta-sarcoglycan. *Muscle Nerve* **29**, 409-419.

Stamler, J. S. and Meissner, G. (2001). Physiology of nitric oxide in skeletal muscle. *Physiol. Rev.* **81**, 209-237.

Stillwell, E., Vitale, J., Zhao, Q., Beck, A., Schneider, J., Khadim, F., Elson, G., Altaf, A., Yehia, G., Dong, J. H. et al. (2009). Blastocyst injection of wild type embryonic stem cells induces global corrections in mdx mice. *PLoS ONE* **4**, e4759.

Straub, V. and Campbell, K. P. (1997). Muscular dystrophies and the dystrophin-glycoprotein complex. *Curr. Opin. Neurol.* **10**, 168-175.

Tian, C., Lu, Y., Gilbert, R. and Karpati, G. (2008). Differentiation of murine embryonic stem cells in skeletal muscles of mice. *Cell Transplant.* **17**, 325-335.

Willmann, R., Possekel, S., Dubach-Powell, J., Meier, T. and Ruegg, M. A. (2009). Mammalian animal models for Duchenne muscular dystrophy. *Neuromuscul. Disord.* **19**, 241-249.

Zhao, Q., Beck, A., Vitale, J. M., Schneider, J. S., Terzic, A. and Fraidenraich, D. (2010). Rescue of developmental defects by blastocyst stem cell injection: towards elucidation of neomorphic corrective pathways. *J. Cardiovasc. Transl. Res.* **3**, 66.

Zhou, L. and Zhu, D. Y. (2009). Neuronal nitric oxide synthase: structure, subcellular localization, regulation, and clinical implications. *Nitric Oxide* **20**, 223-230.

Journal of Cell Science